PAPR Reduction and BER Improvement for OFDM System using WH Transform and Data Grouping Technique

Hyung-Yun Kong, Ho Van Khuong

Department of Electrical Engineering, University of Ulsan

e-mail : hkong@mail.ulsan.ac.kr, khuongho2001@yahoo.com, duheeya@mail.ulsan.ac.kr

Abstract

In this paper, we propose a novel OFDM-based system structure to reduce PAPR (Peak-to-Average Power Ratio) and improve BER for OFDM system in which BER enhancement is obtainable based on WH (Walsh-Hadamard) transform to transmit concurrently each data symbol on all subcarriers so as to take advantage of frequency diversity and remedy the effect of channel's frequency-selectivity. By doing so, we also attain a low PAPR. Moreover, DGT (Data Grouping Technique) that is independent on the side information is also applied to further reduce PAPR. The simulation programs have been also performed to verify the validity of the proposed system.

1. Introduction

Communication channel makes signal pulses broadened in time as they travel through the channel (multi-path effect), leading to Inter-Symbol Interference (ISI). The pulse spread restricts the speed at which adjacent data pulses can be sent without overlap, thus limiting the maximum information rate of the wireless system. One technique to avoid the detrimental effect of multi-path, without sacrificing the transmission rate, is OFDM (Orthogonal Frequency Division Multiplexing) modulation [1]. This is a parallel transmission scheme, where the overall frequency band is divided into a number of subbands with separate subcarriers. On each subcarrier, the modulated symbol rate is low in comparison to the channel delay spread, thus ISI can be prevented. Moreover, such subdivision makes OFDM technique attain high spectral efficiency and robustness against frequency selective multi-path fading. Therefore, it is obviously one of competitive candidates for the next generation communication systems to obtain high bit-rate without increasing the transmission bandwidth as well as decreasing the required BER performance so as to meet a drastically increasing demand of information, communication and entertainment services such as voice, data and video, etc which can be accessed anywhere at anytime. However, OFDM adversely suffers some performance degradations. First, it has a high PAPR that tends to lessen the power efficiency of the RF amplifier. Many PAPR reducing techniques have been suggested [1] such as signal distortion techniques, typically clipping, peak windowing and peak cancellation; coding techniques, SLM (Selected Mapping Method) and PTS (Partial Transmit Sequence). In general, applying these techniques is a cost of increasing transmission bandwidth, deteriorating system's performance and making system more complicated. Second, for the channel with frequency-selectivity, error bits occur as their subcarriers experience deep fades in the frequency spectrum. Although this obstacle can be solved in part by using forward error-correction (FEC) codes such as convolutional code or block code, the frequency utilization efficiency is decreased. In order to correct two above shortcomings of the conventional OFDM (C-OFDM) system, we propose a combination of WH transform and DGT before the multi-carrier modulation. The nature of WH transform is to send one data symbol on all subcarriers concurrently to make the frequency diversity benefit at most. As a consequence, in addition to achieving high performance and avoiding the frequency selectivity of the channel, the suggested system can reduce PAPR because the orthogonality of spreading codes guarantees the probability that all subcarriers combine constructively is very small. For further PAPR decreasing improvement, we apply DGT whose aim is to choose a proper set of phase control gains for groups to attain a lowest PAPR before transmitting the signal over the channel without embedding the side information (SI) of phase set into transmitted data and thus, system performance is independent on SI. This is the proposed technique's prominent advantage over SLM and PTS whose SI has an adverse effect on system performance if it is not correctly recovered.

2. Proposed System Structure (P-OFDM)

2.1 Transmitter model

The suggested system block diagram is shown in Fig. 1. First of all, the i^{th} data block of modulated symbols with symbol duration T_S is serial-to-parallel converted into I branches which is subdivided into M groups of length L-1, except the first group of size L, namely B_m where $m=1,\ldots,M$ as in Fig. 2. Then the groups with indices from 2 to M are added one more symbol b_m ($m=1,\ldots, M$-1) taken from the optimizer to produce a lowest PAPR among its all possible combinations of vector $\mathrm{b}=[\mathrm{b}_1\ \mathrm{b}_2\ \ldots\ \mathrm{b}_{M-1}]$. Here, the symbols b_m have no

meaning at the receiver because the purpose of inserting b_m into useful data is only to control the phase of transmitted signal. Therefore, PAPR reduction is paid only for the decrease in spectral efficiency. Compared to the system without using the PAPR reducing technique, that is, all groups consisting of L data symbols, the bandwidth loss of this system is *(M-1)/ML* in which *ML* is chosen to be equal to the number of subcarriers N. If *ML* is large, then the above loss is negligible.

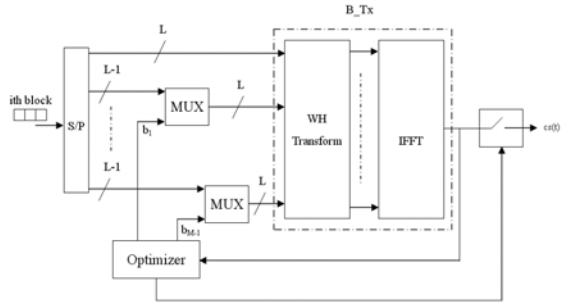

Fig. 1: The first proposed OFDM Transmitter Model

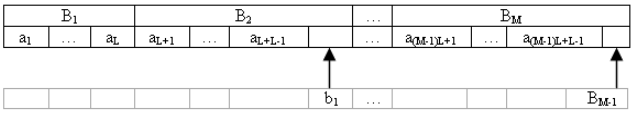

Fig. 2: Structure of M groups (a_u: data symbols, b_m: phase control factors)

We denote the input vector and output vector of WH transform block by a and w, respectively

$$a = [a_1\ a_2\ \dots\ a_N]^T \quad (1)$$

$$w = d\ a \quad (2)$$

where d is Walsh-Hadamard matrix, each column of which is considered as the spreading code of the symbol a_k in frequency domain.

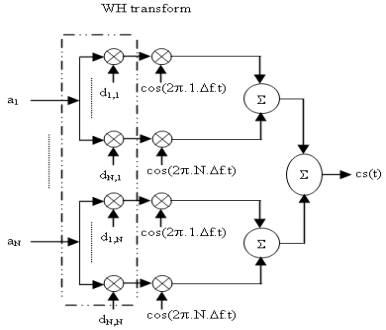

Fig. 3: Detail block diagram of B_Tx

The nature of B_Tx (see Fig. 1) is illustrated in Fig. 3, where each symbol a_k *(k=1,..., N)* is replicated N times and multiplied with $d_{n,k}$ *(n=1,..., N)*. The resulting signal is given below:

$$u_{n,k} = a_k d_{n,k}, \mathrm{n} = 1,...,N, \mathrm{k} = 1,...,N \quad (3)$$

where $d_{n,k}$ is the n^{th} chip of the k^{th} spreading code and a_k denotes the k^{th} symbol. Then, these $u_{n,k}$ are multi-carrier modulated by N subcarriers with frequencies chosen to be an integer multiple of block rate. In this system, we adopt $\Delta f = 1/NT_S$ in which Δf describes the frequency distance between two adjacent subcarriers and the selecting Δf as above assures that all subcarriers are orthogonal. This is a mandatory condition for an OFDM system.

Subsequently, the signals from all parallel branches after spread in frequency domain by d_k are summed together which results in a composite signal as follows

$$cs(t) = \sum_{i=-\infty}^{\infty} \sum_{k=1}^{N} \sum_{n=1}^{N} A a_k(i) d_{n,k} \cos(2\pi n \Delta f t) p(t - iNT_s) \quad (4)$$

where $p(t)$ is a unit-amplitude rectangle pulse over the interval $[0,NT_S]$; A: the amplitude of each sinusoid signal; i: the i^{th} block.

In practice, multi-carrier modulation block can be implemented efficiently by IFFT (Inverse Fast Fourier Transform). Therefore, the whole block diagram of Fig. 3 can be replaced by a WH transform followed by IFFT as in Fig. 1.

As usual, N-point IFFT is used to perform multi-carrier modulation which is equivalent to the sampling the continuous signal $cs(t)$ with the sampling period $1/N\Delta f$. However, this sampling period is not short enough to capture the peaks of the signal $cs(t)$ and thus leading to the large error in computing PAPR compared to the true PAPR value. Therefore, to increase the degree of accuracy of calculated PAPR, we follow [2] that ensures the computed PAPR to be almost approximate with the continuous PAPR value by applying oversampling with a factor of greater than four. In this paper, the signal is oversampled by a factor of 8. Therefore, the sampling duration is given by $T_{sampling} = T_S/8$.

To implement this intention by IFFT, we pad $7N$ zero samples at the tail of vector w and take 8N-point IFFT on the resulting vector to have the signal $cs(nT_{sampling})$ in the discrete form which is used to calculate the PAPR defined as

$$PAPR = \frac{\max\limits_{0 \le m < 8N} \left| cs\left(mT_{sampling}\right) \right|^2}{\underset{0 \le m < 8N}{mean} \left| cs\left(mT_{sampling}\right) \right|^2} \quad (5)$$

where $cs(mT_{sampling})$ is the transmitted signal during one OFDM symbol. For the C-OFDM, PAPR can reach the maximum value of N in the worst case as all subcarriers combine coherently.

The above PAPR is computed for all possible combinations of vector b and stored in the buffer of the optimizer. When the PAPR computation is finished, the optimizer selects an optimal combination of b corresponding to the lowest PAPR and turns the switch on to send $cs(t)$ to the next block.

One of OFDM system's outstanding advantages is capability of suppressing completely ISI caused by multi-path dispersion channel. This is validated by inserting a guard interval Δ with length greater than the maximum delay spread of the channel. Although this interval reduces the spectral efficiency, the complexity of receiver is significantly decreased. Finally, the integrated signal $cs(t)$ is transmitted after RF-up conversion.

2.1.2. Channel Model

If the condition $\Delta f << B_C << BW$ (B_C: coherent bandwidth of channel, BW: total bandwidth of system) is satisfied, then each subcarrier only undergoes a flat fading. Therefore, the frequency-selective Rayleigh fading channel's transfer function H_n can be modeled as $H_n = \alpha_n \exp(j\phi_n)$, where α_n is the amplitude and ϕ_n the phase in the n^{th} subchannel or the n^{th} subcarrier due to fade; α_n are statistically independent Rayleigh random variables and ϕ_n are uniform random variables over the interval $[0,2\pi]$. In this paper, α_n and ϕ_n are assumed to be unchanged during each symbol interval but fluctuate over longer periods of time.

2.1.3 Receiver model

The received signal after frequency down-converted, guard-interval removed and analog-to-digital transformed is processed sequentially as shown in Fig. 4. First, the discrete signal *r(m)* given by

$$r(m) = \sum_{k=1}^{N}\sum_{n=1}^{N} A\alpha_n e^{\phi n} e^{j2\pi n\Delta f m T} a_k d_{n,k} + v(m) \qquad (6)$$

is N-point fast Fourier transformed for multi-carrier demodulation, where α_n and ϕ_n are in (7); *v(m)* is a AWGN component with zero mean and variance σ_n^2; *T*: sampling period.

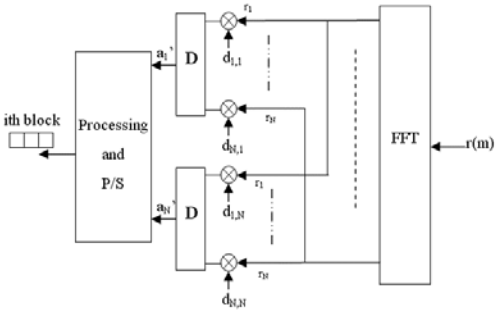

Fig. 4: Block diagram of the proposed OFDM receiver

The resultant signal *r* is of the following form with an assumption that the frequency synchronization is perfect:

$$\underbrace{\begin{bmatrix} r_1 \\ \mathrm{M} \\ r_N \end{bmatrix}}_{r} = Ad \underbrace{\begin{bmatrix} a_1 \\ \mathrm{M} \\ a_N \end{bmatrix}}_{a} \otimes \underbrace{\begin{bmatrix} H_1 \\ \mathrm{M} \\ H_N \end{bmatrix}}_{H} + \underbrace{\begin{bmatrix} V_1 \\ \mathrm{M} \\ V_N \end{bmatrix}}_{V} \qquad (7)$$

where

$$r_n = \sum_{k=1}^{N} A\alpha_n e^{j\phi n} a_k d_{n,k} + V_n \quad , \mathrm{n}=1,\ldots,\mathrm{N} \qquad (8)$$

and noise vector $V=[V_1\ V_2\ \ldots\ V_N]^T$ is FFT of $v=[v(1)\ v(2)\ \ldots\ v(N)]^T$; $(.)^T$: transpose operator; *d:* Walsh-Hadamard matrix; *a*: vector of the original data symbols; ⊗: element-by-element product; *H*: matrix of channel coefficients.

Eq. (7) shows that there is interference among data symbols, called IDSI, which degrades the performance of the system.

Before the a_k is decoded, *r* is despread by its own codes $d_k = [d_{1,k}, d_{2,k},\ldots, d_{N,k}]^T$ to produce a vector:

$$y_k = [y_{1,k}, y_{2,k},\ldots, y_{N,k}]^T = r \otimes d_k \qquad (9)$$

Then, we apply the MMSE (Minimum Mean Square Error) condition [4] on y_k to recover a_k as follows

$$a'_k = \sum_{n=1}^{N} e_n y_{n,k} \qquad (10)$$

where e_n are combination coefficients given by [4]:

$$e_n = \frac{H_n^*}{|H_n|^2 + 1/SNR_M} \qquad (11)$$

in which SNR_M is signal-to-noise power ratio.

It is straightforward to infer from Eq. (11) that MMSE detector minimizes the IDSI and Gaussian noise while best exploiting the frequency diversity benefits.

Finally, the detected symbols a'_k are passed through a processing block and parallel-to-serial transformed to recover the original data block. The function of the processing block is to simply remove the last bits of the recovered data blocks with indices greater than 2. Therefore, the *SI* has no effect on the system's performance. This is a prominent feature of DGT over other PAPR-reducing techniques such as PTS and SLM which strongly depend on *SI*.

3. Simulation results and discussions

To be convenient for the goal of comparison between P-OFDM and C-OFDM, computer simulations only examine the MMSE detectors in the propagation environment of AWGN plus frequency selective Rayleigh fading. Moreover, the original data is assumed to be BPSK-modulated and each element of the phase control vector *b* is selected from the set {-1, +1}. Furthermore, the number of subcarriers is limited to N=16 and 32 for low computation complexity.

P-OFDM	Mean	Variance	Max	Min
N=16-1	2.5820	0.3142	6.1594	1
N=16-2	2.2959	0.1437	4.5011	1
N=16-4	1.9961	0.0656	3.7169	1
N=16-8	1.6732	0.0521	2.2659	1
N=32-1	3.2316	0.4708	8.2103	1.6928
N=32-2	2.9647	0.2894	7.0368	1.6173
N=32-4	2.6237	0.1628	6.7106	1.5569
N=32-8	2.2725	0.1183	6.1221	1
C-OFDM	Mean	Variance	Max	Min
N=16	3.7102	1.3295	16.0000	1.7071
N=32	4.3643	1.4969	18.0000	1.9321

Table 1. PAPR's parameters comparison for C-OFDM and P-OFDM (N=32-2 means 32 subcarriers and 2 groups)

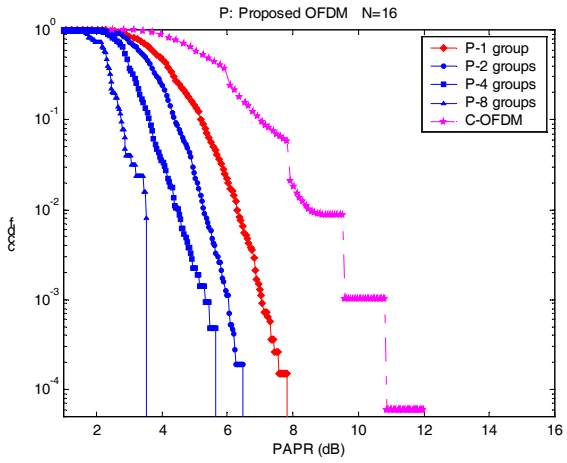

Fig. 5: ccdf of PAPR for C-OFDM and P-OFDM (ccdf=Pr[PAPR>$PAPR_0$])

The statistical data of PAPR for the different number of subcarriers N=16, 32 is illustrated in Table 1 in which PAPR is calculated for 500000 data symbol combinations whose components are randomly selected with a uniform possibility and the sample number per an OFDM symbol is 8N. Moreover, the group number under investigation is M=1, 2, 4 and 8. For any value of *N* and *M*, the PAPR of the proposed system is considerably better than that of C-OFDM, particularly, its PAPRs fluctuate slightly around the mean value (small variance), for example: P-OFDM's average PAPR is 2.9647 (N=32-2) while 4.3643 for C-OFDM and P-OFDM's PAPR variance is 0.2894 in contrary to 1.4969 for C-OFDM. Furthermore, other parameters such as maximum PAPR and minimum PAPR are considerably less than those of C-OFDM. Table 1 also shows that PAPR's parameters increase with respect to an increase of *N*. With small variance, the new system demonstrates that its PAPR is less sensitive with input data combinations than C-OFDM and changes

almost slowly. Finally, the more groups the input data is divided into, the more effective the PAPR reduction. For P-OFDM, the probability that PAPR is greater than 6.1221 is zero for the case of 32 subcarriers and 8 groups; and similarly 2.2659 for N=16 and M=8. However, the cost to be paid for this improvement in PAPR is the bandwidth waste but BER performance is not degraded because it is not dependent of SI (see Figs. 7-8).

In order to have an insightful and intuitive view on PAPR statistics, Figs. 5-6 plot ccdf (complementary cumulative density function) of PAPR for N=16, 32 for M=1, 2, 4, 8 groups. Once again these figures reveal a dramatic improvement in alleviating a high PAPR in the new system over C-OFDM. For instance, a PAPR reducing enhancement of the P-OFDM is about 3 times at ccdf 10^{-4} over C-OFDM for N=16 and M=2.

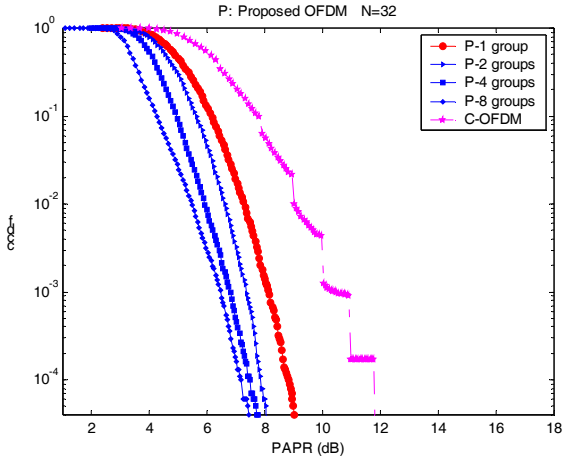

Fig. 6: ccdf of PAPR for C-OFDM and P-OFDM

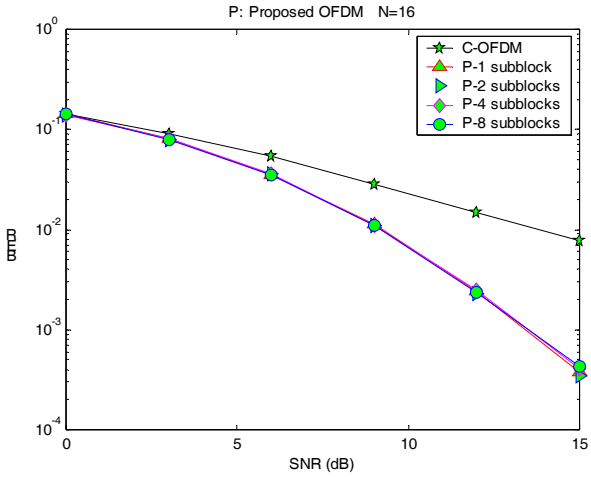

Fig. 7: Performance of C-OFDM and P-OFDM for N=16

BER performance in frequency selective Rayleigh fading channel with AWGN illustrated in Figs 7-8 shows that the performance of C-OFDM is significantly degraded by fading channel. However, for P-OFDM, due to frequency diversity benefit, its performance is considerably improved in comparison to C-OFDM with approximately 5dB SNR gain at BER 10^{-2} for any N and M. Furthermore, BER enhancement accelerates with respect to an increase in the subcarrier number while C-OFDM's BER is almost unchanged. This is because the flat fading property on each subcarrier is guaranteed better as the total transmission bandwidth is subdivided into many narrower frequency-bands and frequency diversity gain also increases according to N. Obviously, this property can not be found in C-OFDM. Figs. 7-8 also demonstrate that there is no performance degradation for P-OFDM as the number of groups increases because as reasoned in part 2.1 that P-OFDM's performance is independent on the number of groups.

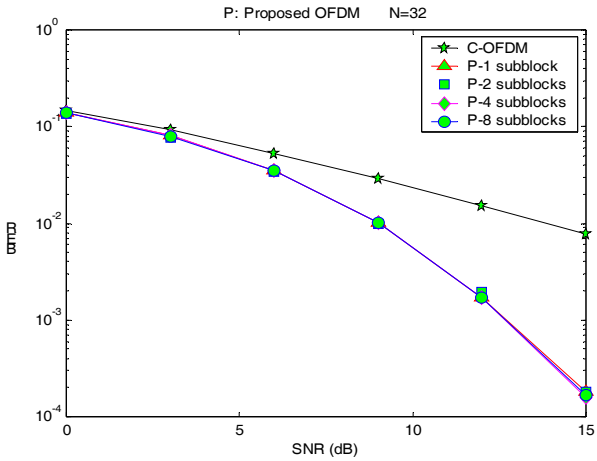

Fig. 8: Performance of C-OFDM and P-OFDM for N=32

4. Conclusion

The proposed system offers an orthogonality between data symbols and a frequency diversity gain. Therefore, it achieves a low PAPR and a high performance over C-OFDM, especially, the additional BER improvement as the number of subcarriers and SNR increase. Moreover, PAPR can be further reduced by subdividing the input symbol stream into smaller groups. The larger the number of groups, the more PAPR reduction increases and the less bandwidth utilization efficiency but not deteriorate BER performance. Therefore, our systems are suitable to apply for the transmitters of high frequency amplifiers with small dynamic range and operated in harsh environments as multi-path fading channels.

References

[1] Richard van Nee, Ramjee Prasad, "OFDM for Wireless Multimedia Communications", Artech House, 2000.

[2] C. Tellambura, "Computation of the Continuous-Time PAR of an OFDM Signal with BPSK Subcarriers", IEEE Communications Letters, Vol. 5, pp.185–187, May 2001.

[3] James K. Cavers, "Mobile Channel Characteristics", Kluwer Academic Publishers, 2000.

[4] D.N. Kalofonos, M. Stajanovic, J.G. Proakis, "On the performance of Adaptive MMSE Detectors for a MC-CDMA System in Fast Fading Rayleigh Channels", The ninth IEEE International Symposium on Personal, Indoor and Mobile Radio Communications, Vol. 3, pp. 1309–1313, 8-11 Sept. 1998.